POWER LAW MODEL ADAPTATION TO FINGERING OF NON-NEWTONIAN FLUIDS

Michelle Hine, Yusuke Shimabukuro, and Amy Veprauskas

Abstract

The growth rate of fingers of a Newtonian fluid can be modeled by a power law dependence on time. In this experiment, we examine whether the model can be adapted to describe a fluid with changing viscosity. We provide two possible interpretations. For PVA and a PVA/glycerol solution, we show that by assuming a constant exponent, the changing behavior of the fluid can be captured by a coefficient that changes with time. In addition, because the PVA/glycerol solution exhibits dual behavior matching both the Newtonian and non-Newtonian fluids, we propose a piecewise model of two power laws to capture both behaviors.

1. Introduction

When fluid flows down an inclined plane as a result of gravity, it initially retains a uniform front, also called a contact line, that is perpendicular to the direction of flow. The front then develops an instability, either taking a sawtooth form or, more commonly, developing fingers [3]. These three flows are depicted in Figure 1. Experiments have shown that making a fluid viscoplastic could help avoid fingering [1].

Figure 1. The three fluid flows.

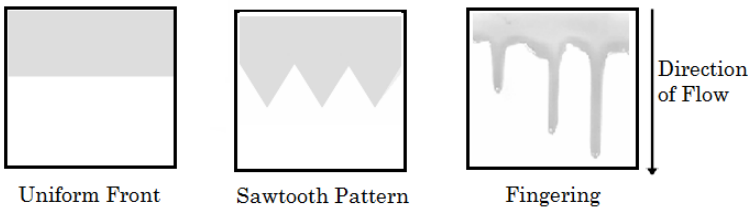

Fluid flow down an inclined plane has been studied extensively, particularly for Newtonian fluids. It is generally accepted that fingering is caused by an imbalance of the opposing forces of gravity and surface tension. When a fluid is placed on an inclined surface, the front of the fluid experiences the competing forces of gravity driving the fluid down the incline and surface tension holding the fluid in place. This combination of forces causes the contact line to develop a ridge, as can be seen in Figure 2. When the ridge becomes sufficiently thick, the force of gravity causes an instability which can result in the development of fingers. It is commonly observed that any fingering instability along the front develops at the same time [1]. The fingering of fluid flow is especially relevant to industrial processes that require a surface to receive an even coating of fluid.

FIGURE 2. Side view of ridge developing in a fluid contact line.

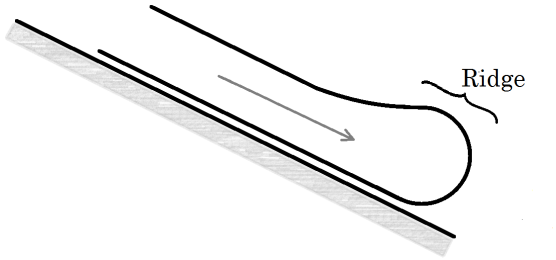

In this paper we examine the growth rate of fingers for both a Newtonian and a non-Newtonian fluid down an inclined plane. For the Newtonian fluid, we consider a glycerol solution, because it is a relatively inexpensive yet well-studied fluid with established properties. For the non-Newtonian fluid, we use a polyvinyl alcohol (PVA) solution. In order to better understand the difference in Newtonian and non-Newtonian fluids, we also study a mixed solution of 50% glycerol and 50% PVA by volume. This combination of solutions is commonly used by biologists to mount slide specimens [4].

Non-Newtonian fluids do not obey the Newtonian relationship between sheer stress and shear rate. PVA is a dilatant, or shear-thickening, non-Newtonian fluid. Dilatant fluids exhibit an increased viscosity under shear stress. As PVA flows down the inclined plane, the acceleration of the fluid increases shear stress. The PVA/glycerol solution contains both Newtonian and non-Newtonian fluids, and acts in a non-Newtonian manner. However, when the PVA/glycerin solution first starts to flow, the fluid has a lower velocity so it behaves more like the glycerol.

Jerret and de Bruyn have established a power-law time dependence model governing the growth rate of the fingers of a Newtonian fluid [3]. Through experimental measurements we adapt this model to a non-Newtonian fluid.

2. METHODS

2.1. **Experimental Apparatus and Setup.** In this experiment we used was a glass plane with dimensions of length 29.21 cm x width 28.26 cm. Before every run, the surface was thoroughly cleaned and dried. The glass was attached to a metal frame, hinged at one end to allow for varying angles. The angle of inclination was controlled by a variable support at the other end. The support had two settings; one set to make the surface level and the other set to give a certain incline angle. The measurements of the angles were accurate up to $\pm 0.1^\circ$, measured with an electronic level. The data was collected by a video camera, which was attached vertically at the top of the metal frame so that it remained perpendicular to the glass surface to avoid parallax error. The apparatus is shown in Figure 3.

We used three different fluids: a 3:1 solution of glycerol to water with a concentration of 1.5 grams of scarlet red procion dye per liter solution, PVA with green dye commercially produced by Rexco[1], and a 1:1 mix of these glycerol and PVA solutions. The dyes improved the contrast between the fluids and the glass plane, allowing the normally clear fluids to be better captured on camera.

[1] The PVA consists of concentration $56-67\%$ water, $31-34\%$ ethyl alcohol, $7-8\%$ acetic acid ethanol ester, polymer with ethanol, and $1-2\%$ butyl alcohol.

FIGURE 3. Apparatus. The arrow denotes removal of the dam used for the fluid front.

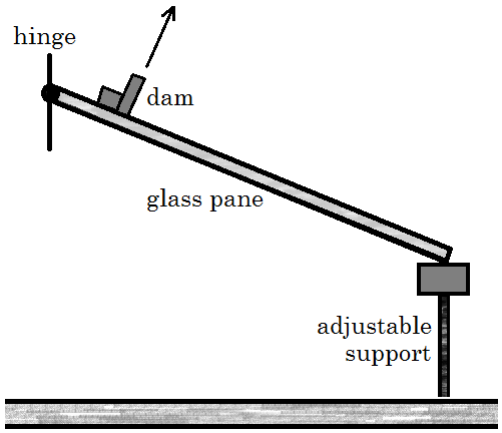

PVA has properties of film forming and adhesiveness, and is widely used in various applications, such as a thickener, stabilizer and binder. PVA has a much higher wetting tendency than glycerol; after stabilizing on a flat glass surface, the PVA solution had a contact angle of 9.4° while glycerol had a contact angle of 23.5°. The PVA/glycerol solution exhibits behavior closer to that of the PVA, spreading out to a similar distance, but with a contact angle of 12.2°.

We examined two different initial shapes for the fluids before inclining the plane. We placed the fluid both as large circular drops on the glass surface and also behind a dam so that it started with a uniform fluid front, as can be seen in Figures 4 and 5. The dam had metal brackets held in place with magnets to make the initial shape of the fluid rectangular, with a fixed width of 20 cm, as shown in Figure 6. In both cases, the glass began at a zero angle for initial fluid placement. The dam was lifted before inclining the glass. A volume of 3 mL of fluid was used for the large circular drops and two angles were tested, 10° and 20°. The radii of these drops ranged from 3.5 cm for the PVA to 2.9 cm for the glycerol. A volume of 5 mL of fluid was used with the dam and only the 20° angle was tested. We conducted multiple trials at each angle. The finger length is defined to be the distance between the tip of finger and the original position of the instability, as illustrated in Figure 9, and measurements were made using ImageJ[2] to process stills from the video captured. For glycerol we were able to convert the stills to binary. With these images we used the macro given in Appendix A to automate the measurements. For the fluid front, we measured the finger growth of multiple fingers.

The decision to examine two different initial shapes was motivated by differences observed between the fluid flow in the two methods. When fingering develops in a fluid front, some fingers will be longer than others. This problem is exaggerated when the fluid volume is not evenly distributed. The brackets on the dam constrained the fluid to a mostly rectangular shape. This helped to regularize the experiment, though we still did not have a completely even distribution of the fluid. When the liquid began in circular form, only one finger developed, thus eliminating the irregularity observed in the other method. However, the

[2] `http://rsbweb.nih.gov/ij/`

FIGURE 4. Large circular drops.

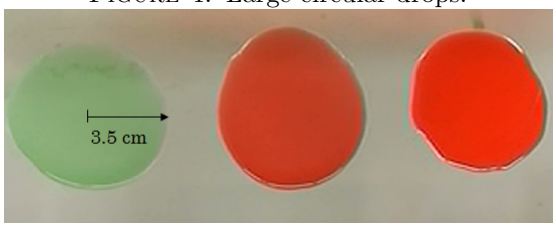

FIGURE 5. Fluid front.

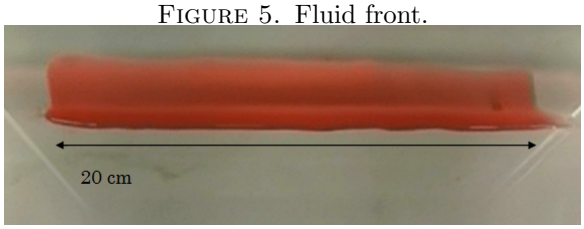

FIGURE 6. Rear of dam depicting magnetically held brackets.

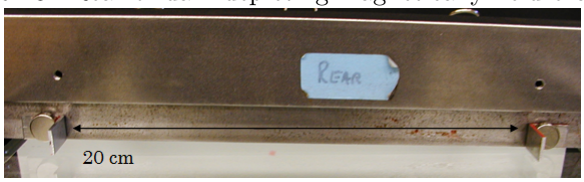

non-Newtonian behavior of PVA and the PVA/glycerol solution were more noticeable with the fluid front. With the fluid front, both PVA and the PVA/glycerol solution initially sped up quickly, as seen in Figure 8. Soon after, the speed decreased due to the non-Newtonian characteristics of PVA. This indicates that for a non-Newtonian fluid, more fluid may result in higher shear stress.

When the fluids began in circular form, regardless of the incline angle, the PVA flowed most quickly, followed by the PVA/glycerol solution; see Figure 7. For the fluid front profile, we observed a switch–the PVA/glycerol solution flowed most quickly, followed by the PVA, as in Figure 8. For a Newtonian fluid, increased volume increases how fast the fluid will flow. Hence, for the PVA/glycerol solution we saw that the non-Newtonian characteristics of the fluid had less influence on the flow than the volume. In both cases, the glycerol flowed the slowest. With the dam, we observed seven to nine fingers for both the PVA and the PVA/glycerol solution. For glycerol, we observed five to six. The fingers of the glycerol were also notably wider than the fingers of the other fluids.

2.2. **Theoretical Model.** For a Newtonian fluid, Jerret and de Bruyn modeled the finger growth using the power law dependence on time [3]:

$$x_d = A(t - t_0)^{\beta}. \tag{1}$$

Variable x_d is the downslope tip position after the instability as shown in Figure 9. Thus, x_d measures the distance between the tip of a finger and the original position at the beginning

FIGURE 7. A typical run of the large circular drops at an angle of 20°.

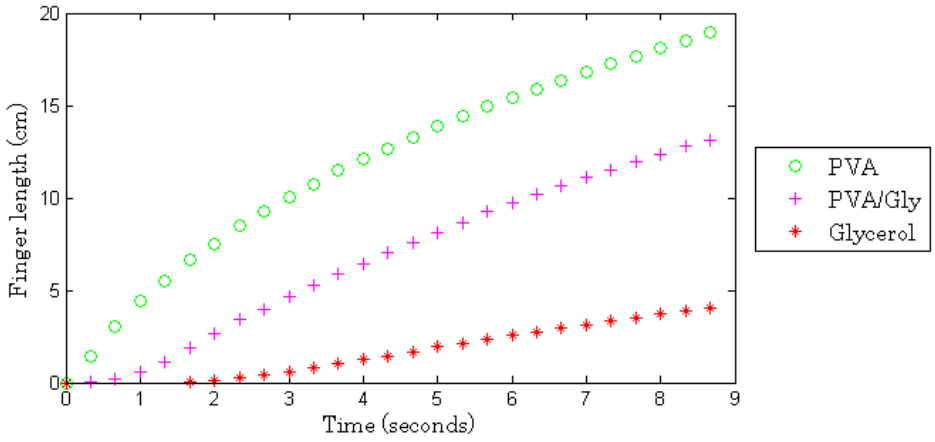

FIGURE 8. Typical runs of the fluid fronts at an angle of 20°.

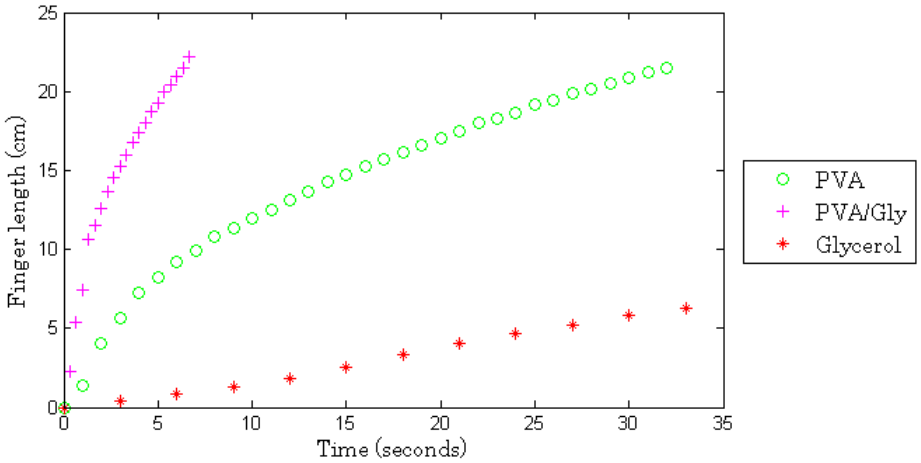

of the instability. This quantity is measured directly from the experiment. The amplitude of the fingering A, and the exponent characterizing finger growth rate β are free parameters used to fit the data. The parameter t_0 is the time that the instability develops.

Jerret and de Bruyn obtained this model based on experimental data. Their experiment used a known volume of Newtonian fluid (glycerol, heavy mineral oil, and light mineral oil) poured behind a gate, very similar to our experimental setup. Jerret and de Bruyn noted that accounting for experimental uncertainties, for both the glycerol and the oils, β is independent of the incline angle. Because β was equal (within a margin of error) for the two mineral oils, Jerret and de Bruyn believe that the growth exponent is independent of

FIGURE 9. Variable x_d, measuring the distance between the tip of a finger and the original beginning of the instability.

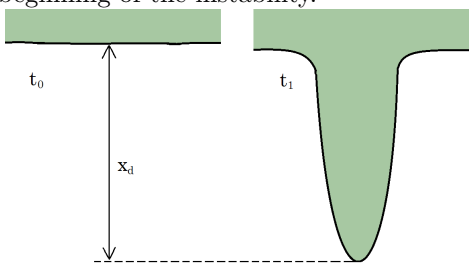

viscosity. Also, for all three fluids, the amplitude equation is:

$$A = k\sin(\alpha), \tag{2}$$

where α is the incline angle, and k is inversely proportional to fluid viscosity. Hence the amplitude of fingering depends on the angle and increases with decreasing viscosity.

From theoretical calculations supported by experimental data, Huppert found that before fingering occurs, the front advances proportionally to $t^{1/3}$ [2]. Jerret and de Bruyn noted that both the values for β and A agreed well with the parameters characterizing the fluid motion after the instability. For the most part, their pre-instability data fit the model, but with a β of a value higher than the expected 1/3. During Jerret and de Bruyn's experiment, the contact line seemed to approach a $t^{1/3}$ behavior, but only after a supercritical growth time. Also, they only observed the $t^{1/3}$ growth rate for the smallest angles studied. Jerret and Bruyn argue that the discrepancy between their experiment and Huppert's model results because for angles $\gtrsim 5°$, fingering occurs before the initial growth rate has approached the $t^{1/3}$ time-dependent behavior.

We propose that it is possible to adapt this model for a non-Newtonian fluid. However, since the viscosity of PVA will increase with velocity, it is necessary to make the amplitude time dependent. The model, given in equation (1), becomes

$$x_d = A(t)(t - t_0)^{\beta} \tag{3}$$

where, x_d, β, and t_0, are as before, free parameters used to fit the data. The viscosity for each solution should be a non-decreasing function of time. Since amplitude is inversely proportional to viscosity, the function $A(t)$ should be a non-increasing function. Moreover, $A(t)$ should actually decrease with time. We do not expect β to change with time, since Jerret and de Bruyn indicated that growth rate was independent of viscosity.

2.3. **Calculations.** We first fit the data to the power law with constant amplitude. We used the least square fit to find the parameters in the power law. Experimental data was read directly into MATLAB[3] and applied to the least squares routine. By taking the logarithm, the power law can be rewritten as,

$$\log(x_d) = \log(A) + \beta\log(t - t_0),$$

and defining $c = \log(A)$ yields,

$$\log(x_d) = c + \beta\log(t - t_0).$$

[3] MathWorks ® Inc., `www.mathworks.com`; Natick, Massachusetts.

Since x_d and t are given, the equation can be written in the matrix form,

$$QW = B,$$

where Q contains coefficients of c and β, B contains $\log(x_d)$ for each data point, and W contains c and β. The least squares fit is given by

$$W = (Q^T Q)^{-1} Q^T B,$$

where Q^T is the transpose of Q. This yields parameters β and c. Then, A is found by $A = \exp(c)$.

The condition number of the matrix Q was small enough to neglect computational differences between other techniques, such as QR decomposition or SVD.

3. Results

We fit the growth rates of the fingers to the power-law model, assuming that A is constant and letting $t_0 = 0$. Averaging the measurements taken, we arrived at the values for A and β for the large circular drops, given in Tables 1 and 2.

Table 1. Finger growth for large circular drops at a 10° angle.

Fluid	β	A
Glycerol	1.26	0.32
PVA	0.77	2.82
PVA/Glycerol Solution	1.02	1.20

Table 2. Finger liquid drops at a 20° angle.

Fluid	β	A
Glycerol	1.09	0.53
PVA	0.84	3.60
PVA/Glycerol Solution	1.38	0.51

We compare these values to the assumptions of the model. Since β is independent of incline angle we expect that, for each fluid, β is the same for both angles. For glycerol and PVA, we see that this is true up to ≤ 0.15, while it is off by twice as much for the PVA/glycerol solution. Since A is defined by $A = k\sin(\alpha)$, where α is the angle, we expect that k should be the same for the two angles. We know that $\sin(10°) \approx \frac{1}{2}\sin(20°)$, so the k value for the 20° angle should be about half the k value for the 10° angle. Physically, however, this should not be true for the non-Newtonian fluids, because k changes with viscosity. Once again we see that this is clearly not true for the PVA/glycerol solution.

We also calculated A and β for the fluid front. The values are given in Table 3.

Table 3. Finger growth for fluid front at a 20° angle.

Fluid	β	A
Glycerol	0.76	1.03
PVA	0.65	1.28
PVA/Glycerol Solution	0.57	2.46

To give more meaning to these models we examine the graphs of the data with their respective models. Figures 10 and 11 give graphs of the experimental data points along with the best fit models for glycerol, PVA, and the PVA/glycerol solution. Plotting the data from these runs we find that the finger growth of glycerol is initially concave up and the finger growth for the PVA is concave down. Meanwhile, the finger growth for the PVA/glycerol solution switches from concave up to concave down but with a much higher rate than the glycerol. This indicates that a higher velocity needs to be reached before the non-Newtonian characteristics affect the fluid. Comparing Jerret and de Bruyn's power law model $x_d = A(t-t_0)^\beta$ to the data, we see that as expected, this model fits the glycerol well. Meanwhile, the model is not a very good fit for the PVA or the PVA/glycerol solution. For the large circular drops, the model is the worst fit for the PVA/glycerol solution. For the fluid front, it appears to be a much better fit for the PVA/glycerol solution but we believe this is due to the lack of data points from the fluid front.

FIGURE 10. Finger growth with power law models for the large circular drops at a 20° angle.

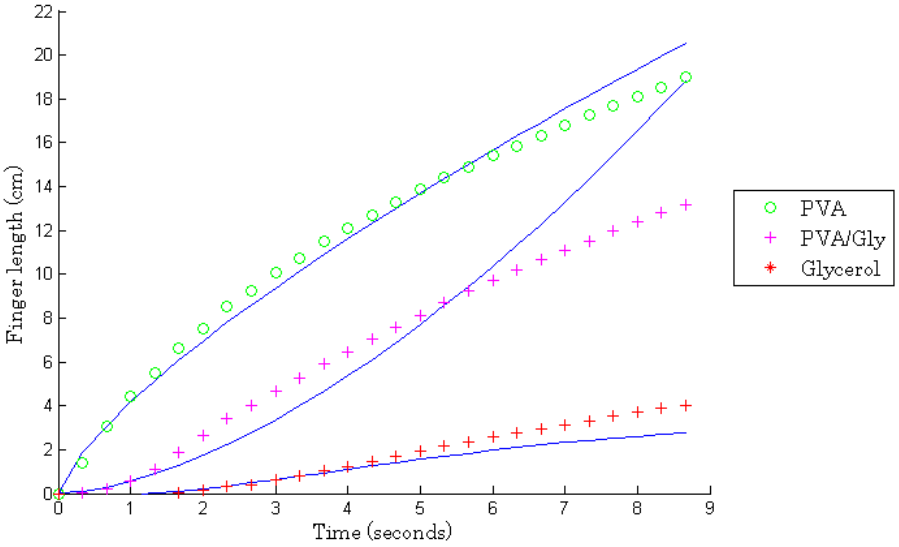

It is clear that the power law model does not fit the data for the non-Newtonian fluids well because the initial fast finger growth at the beginning dramatically decreases to nearly linear growth. This indicates that, after a critical time, the power law would be a good fit for the non-Newtonian fluid.

Further, while we might have expected the model to fit the PVA/glycerol solution better than the PVA we see that this is not the case. The issue is caused by the shift in concavity as the model must compensate between the two regimes.

The two distinct behaviors for finger growth rates of the non-Newtonian fluids also suggests that we could model the finger growth using a piecewise function of two different power laws, one for the initial faster growth and one for the subsequent slower growth, as discussed in the next section.

FIGURE 11. Finger growth with power law models for the fluid front at a 20° angle

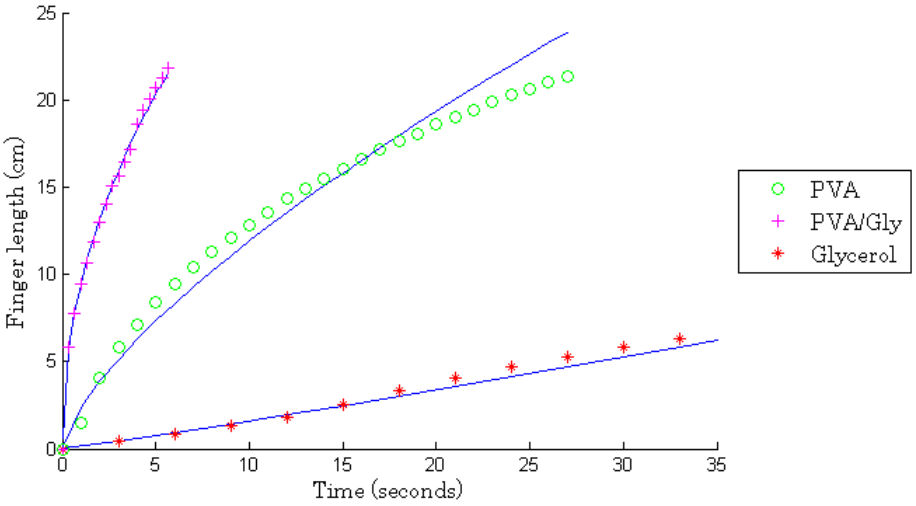

4. Discussion

4.1. **Moving Average for A(t).** For PVA and the PVA/glycerol solution, the power law alone does not explain the movement of the fluid. Because amplitude is a function of time, the model needs to incorporate a changing amplitude. A shear-thickening fluid flowing down an inclined plane should have increasing viscosity from acceleration due to gravity. The increasing velocity creates higher shear forces within the fluid, which in turn increase viscosity. The model is restated below:

$$x_d = A(t)(t - t_0)^{\beta}. \tag{4}$$

From the theory, $A(t)$ should vary inversely with viscosity. Since viscosity of a shear-thickening fluid increases with time, for both the PVA and the PVA/glycerol solution, $A(t)$ should decrease with time.

We implicitly modeled the changing amplitude $A(t)$ by using an iterated least-squares fit of the data. First, we computed the least squares fit of the entire dataset, to obtain β, the power, and a temporary value for A. We then computed a moving average for $A(t)$ by fixing β as the computed value, and running an iterated least-squares process on sets of five data points. The MATLAB code for this iterated process is in Appendix B. For PVA and the PVA/glycerol solution, the values of $A(t)$ do indeed decrease with time.

Figures 12 and 13 show moving average for $A(t)$ for the PVA, and PVA/glycerol solution liquid drops at a 20° angle.

4.2. **Power Law Fit with Breakpoint.** We propose an alternate interpretation for the PVA/glycerol. As noted before, the PVA/glycerol appears to exhibit both Newtonian and non-Newtonian behavior. This suggests that the data might be better explained by a double power law fit–one for each of the dual behaviors. To capture this numerically, we first ran the least-squares fit on split sets of data points, $1,\ldots,j$ and $j,\ldots,m$, with $2 \leq j \leq m-1$, for m differenced data points. Calculating the parameters A and β and the the l^2 fit for

FIGURE 12. Moving average for PVA.

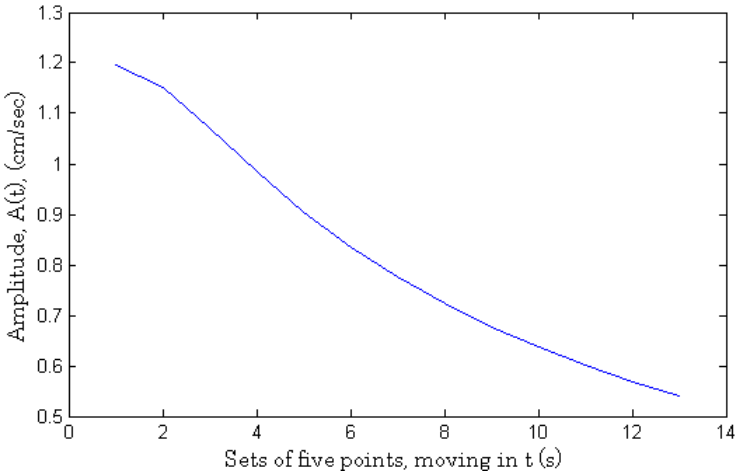

FIGURE 13. Moving average for PVA/glycerol.

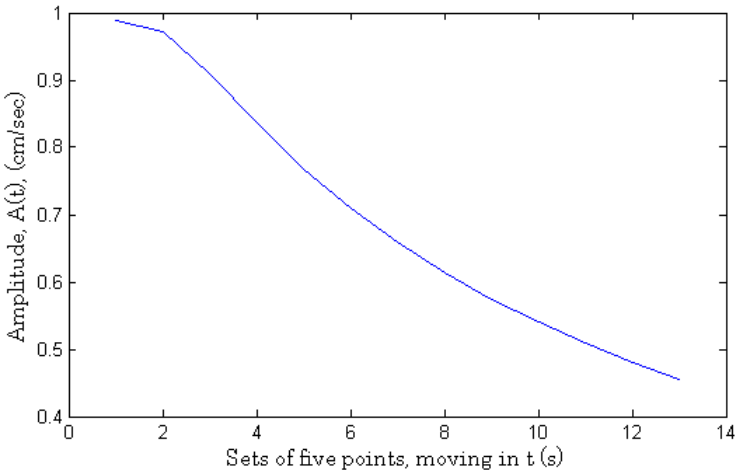

each smaller set of data led to a natural choice of breakpoint. For each set of data, we chose the breakpoint that minimized the combined l^2 norms. The MATLAB code for this can be found in Appendix C. This split model fit the data much better than a single power law model. Figure 14 shows this model for the PVA/glycerol solution fluid front.

4.3. **Growth-Rate Dependence on Volume.** Interestingly, the non-Newtonian behavior of the PVA is much more noticeable for the fluid front than for the liquid drops. For a Newtonian fluid we expect the fluid front at 20° to flow faster than the liquid drop at 20° since there is more fluid. However, for the PVA, the liquid drops flowed faster than the fluid front. It appears that non-Newtonian behavior is governed by the amount of fluid. This could be because more liquid volume allows higher shear forces.

FIGURE 14. Finger growth for the PVA/glycerol solution fluid front with best fit lines for piecewise model.

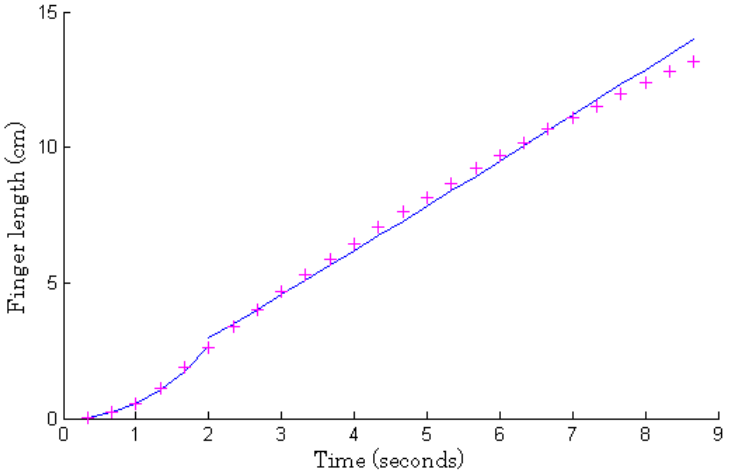

Figure 15 shows the growth rate for PVA with the two different initial set-ups. While both the fluid front and liquid drops for PVA displayed a quick growth followed by a decrease, we saw a more dramatic change in the finger growth for the fluid front. For the PVA/glycerol solution, however, we did not see the same behavior. Instead, the fluid front flowed faster than the liquid drop, as with a Newtonian fluid. Hence, for the PVA/glycerol solution, the volume had more influence than the non-Newtonian characteristics.

FIGURE 15. PVA liquid drops and fluid front at an angle of 20°.

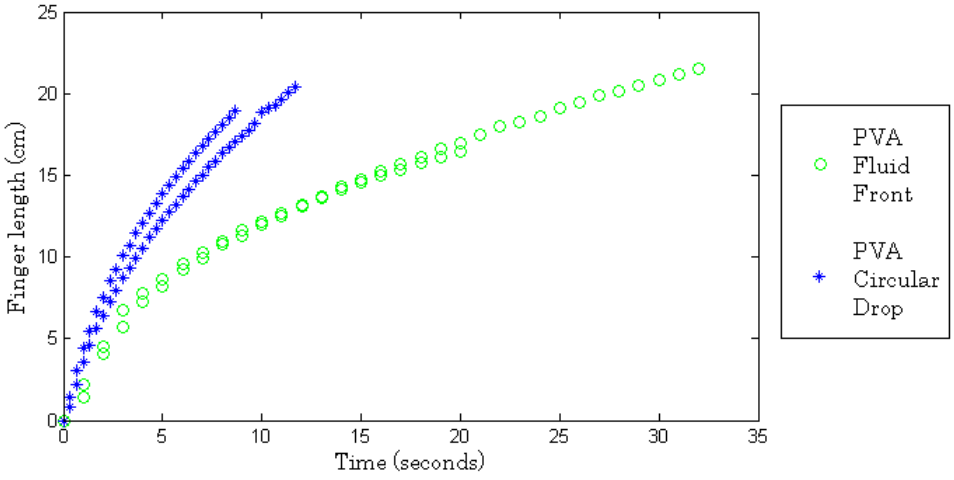

5. Conclusion

Our results show that if the coefficient in Jerret and de Bruyn's model remains constant, then the model is not suitable for fitting the finger growth rate of the PVA and PVA/glycerol solutions. We observe that the finger growth rates of PVA and the PVA/glycerol solutions start off quickly and then slow down to a nearly equilibrium phase in which they behave more like a Newtonian fluid. The increasing viscosity in non-Newtonian solutions is the main factor slowing down the finger growth rate, and the original power law is incapable of describing the non-Newtonian property of the time-varying viscosity.

Variable $A(t)$ in our modified version of the power law captures the behavior of time-dependent viscosity. Our proposed $A(t)$ would be a function decreasing with time and reaching nearly a constant value with increasing time. Using a moving average we showed numerically that this method will likely well-describe the behavior of a non-Newtonian fluid.

Alternatively, we could consider modeling the finger growth rate by a piecewise function of two power laws, one for each regime of the fluid. We showed that this model is a good fir for the finger growth of the PVA/glycerol solution.

6. Future Directions

For further consideration, we suggest experimenting with other non-Newtonian fluids. In addition, it would be useful to obtain a method to measure the viscosity in a dynamic fashion, so that viscosity could be built directly into the model.

We found that the parameter A in the power law varies in time for the non-Newtonian fluids and would like to find an explicit form that fits the finger growth of non-Newtonian fluids. Through studying the time-varying viscosity of a non-Newtonian fluid it may be possible to determine an explicit form of $A(t)$.

Another avenue to explore would be to model the fluid properties governing the drying behavior of the PVA and the PVA/glycerol solutions. Both solutions have differing drying patterns. After sitting for many minutes, PVA forms a film with fractals. The PVA/glycerol solution dries as well, but with a dappling pattern.

Acknowledgements

We would like to thank Dr. Michael Tabor and Mr. Robert Reinking for their continued support throughout the semester.

References

1. S Myers T. Balmforth, N. Ghadge, *Surface tension driven fingering of a visoplastic fluid*, J. Non-Newtonian Fluid Mech. (2007), 142–143.
2. H. E. Huppert, *Flow and instability of a viscous current down a slope*, Nature (1982), no. 300, 427.
3. J.R. Jerret, J.M. de Bruyn, *Fingering instability of a gravitationally driven contact line*, Phys. Fluids A **4** (1992), no. 2, 234–242.
4. Jos Rodriguez and Friedrich Deinhardt, *Preparation of a semipermanent mounting medium for fluorescent antibody studies*, Virology **12** (1960), no. 2, 316–317.

Appendix A

```
// Macro program measures a length between the left endpoint of the fluid and
// the right end of the image in all imported image sequences in ImageJ.
// Imported images must be binary images.
// Program Design: Yusuke Shimabukuro, (C) 2010
```

```
n=nSlices;                          % Take the number of imported images

for (i=1;i<=n;i++){                 % Run from the first image to the last image
setSlice(i);                        % Show the i th image
w=getWidth();h=getHeight();         % Take width and heigth of the i th image
x1=w;
x2=x1;

        for (j=1;j<=w;j++){                         % Scan through all columns
                for (k=1;k<=h;k++){                 % Scan though all rows
                        if(getPixel(j,k)>0){        % Sort out black or white
                                x1=j;               % Store x value in x1
                                if(x1<=x2){
                                        x2=x1;      % Store a current left endpoint
                                        y=k;        % Store a value of y
                                }
                        }
                }
        }
length=w-x2;          % Subtract x2 from width to obtain length
height=h-y;           % Subtract y from height to obtain height of left endpoint
print(length,height); % Print length and height on the log file
}
```

Appendix B

```
% MATLAB program runs least squares for one data set, to calculate a temporary A
% and beta. It then uses beta to calculate the 'moving average' of A(t) for sets
% of five points. Program graphs A(t) against time.
% Program Design: Team AMY, (C) 2010

load data.txt
x=data(1:30,1);

x0=x(1);                % Initial position
diff_x=x(:)-x0;         % Subtract the initial position
diff_x=diff_x(2:end);
[m n]=size(x);
t=[1:m-1]/3;            % Time vector in seconds

Q=ones(m-1,2);          % Create matrix Q for least squares fit
Q(:,2)=log(t);
b=ones(m-1,1);          % Create vector b containing dependent variable
b=log(diff_x);

Qb=Q'*b;                % Run least squares
QQ=Q'*Q;
W=QQ\Qb;
```

```
A=exp(W(1));            % Extract parameters A and beta
beta=W(2);

% Fit A with beta fixed
% A(t-t_0)^beta=x_d, where beta=W(2) calculated from before
A_t=zeros(m-5,1);
for j=1:m-5             % Each time, fit sets of j,...,j+4 components
   newdiff=diff_x(j:j+4);
   tnew=t(j:j+4);
   Q=[tnew.^beta]';
   b=log(newdiff);
   Qb=Q'*b;             % Run least squares
   QQ=Q'*Q;
   W=QQ\Qb;
   A_t(j,1)=W;          % Extract parameter A(t)
end

plot([1:m-5],A_t);      % Plots left to right, points 1-5, 2-6, etc.
title('A(t) vs. t');
xlabel('Sets of five points, moving in t');
ylabel('Amplitude, A(t)');
```

Appendix C

```
% MATLAB program runs least squares for split sets of data, 1,...,j and
% j,...,m-1.  It then minimizes the combined l^2 norm to choose an appropriate
% breakpoint for the data, then graphs the result.
% Program Design: Michelle Hine, (C) 2010

load data.txt
x=data1(1:30,1);

x0=x(1);                    % Initial position
diff_x=x(:)-x0;             % Subtract the initial position
[m n]=size(x);
t=[1:m-1]/3;                % Time vector in seconds

normcompare=zeros(m-2,3);   % Initialize storage for both norms
betas1=zeros(m-2,1);        % Stores beta from beginning fits
Astore1=zeros(m-2,1);       % Stores the A values from beginning fits
betas2=zeros(m-2,1);        % Stores beta from ending fits
Astore2=zeros(m-2,1);       % Stores the A values from ending fits

for j=m-1:-1:2              % Each time, fit first 1,...,j components
    tnew=t(1:j);
    newdiff=diff_x(1:j);
    [A,beta]=leastsquares(tnew,log(newdiff));
    f=A*tnew.^beta;
```

```
    % Store the parameters and norm of (data points - fit)
    betas1(j-1,1)=beta;
    Astore1(j-1,1)=A;
    normcompare(j-1,2)=norm(f'-newdiff);
end

for j=1:m-2                 % Each time, fit last j,...,m-1 components
    tnew=t(j:end);
    newdiff=diff_x(j:end);
    [A,beta]=leastsquares(tnew,log(newdiff));
    f=A*tnew.^beta;
    % Store the parameters and norm of (data points - fit)
    betas2(j,1)=beta;
    Astore2(j,1)=A;
    normcompare(j,3)=norm(f'-newdiff);
    normcompare(j,1)=j;     % Indexes the number of points fit
end

% Choose the index that minimizes the combined l^2 norm
index=1;
minsum=normcompare(1,2)+normcompare(1,3);
for i=2:m-2
    if le(normcompare(i,2)+normcompare(i,3),minsum)
        minsum=normcompare(i,2)+normcompare(i,3);
        index=i;
    end
end

% Plot the new fit line
beta1=betas1(index,1);
A1=Astore1(index,1);
beta2=betas2(index,1);
A2=Astore2(index,1);
f1=A1*t(1:index).^beta1;
f2=A2*t(index:m-1).^beta2;
hold on;
plot(t(1:index),f1,t(1:index),diff_x(1:index));
plot(t(index:m-1),f2,t(index:m-1),diff_x(index:m-1));
xlabel('Time (seconds)');
ylabel('Finger length (cm)');
```